Langmuir

Article

pubs.acs.org/Langmuir

Understanding the Role of H-Bonding in Aqueous Self-Assembly of Two Naphthalene Diimide (NDI)-Conjugated Amphiphiles

Priya Rajdev,* Mijanur Rahaman Molla, and Suhrit Ghosh*

Polymer Science Unit, Indian Association for the Cultivation of Science, Kolkata, India 700032

Supporting Information

ABSTRACT: Supramolecular architectures with the synchronized combination of various directional noncovalent forces are ubiquitous in biological systems. However, reports of such abiotic synthetic systems involving H-bonding in aqueous medium are rare due to the challenge faced in the formation of such structures by overcoming the competition from the water molecules. In this paper we have studied self-assembly of two structurally related naphthalene-diimide (NDI) conjugated bola-amphiphiles (NDI-1 and NDI-2) in water with an aim to realize the specific role of H-bonding among the hydrazide units present in one of the two building blocks (NDI-2) on the self-assembly. Both chromophores showed vesicular assembly in aqueous solution driven primarily by π-stacking among the NDI chromophores, which could be probed by UV−vis absorption spectra. Contrary to common belief, the lack of an H-bonding group in NDI-1 was found to be a boon in disguise in terms of the stability of the aggregates. Whereas NDI-2 aggregates showed LCST around 65−70 °C owing to the breaking of the H-bonds with increased temperature, the NDI-1 aggregates were found to be structurally intact until 90 °C, which may be attributed to the increased hydrophobicity introduced by the absence of the polar hydrazide group. Further concentration- and solvent-dependent UV−vis studies showed that NDI-1 formed assembled structure at greatly dilute solution and also in a solvent such as THF, confirming greater propensity for its self-assembly. As both bola-amphiphiles contain an electron-deficient NDI chromophore, interaction of their vesicles was studied with an externally added electron-rich pyrene derivative. Surprisingly, NDI-1 did not show any charge-transfer interaction with the donor, whereas NDI-2 could effectively intercalate, leading to a functional membrane with tunable surface functionalities. This was attributed to the additional stability of the intercalated state by H-bonding among the hydrazide units.

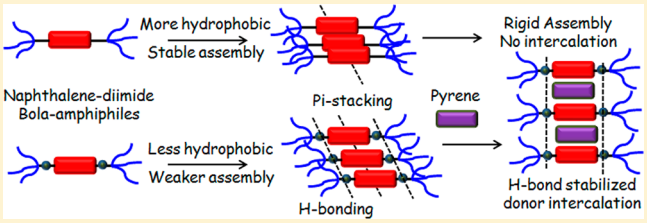

INTRODUCTION

Solvophobically driven aggregation of small-molecule surfactants[1] and amphiphilic macromolecules[2−5] has been studied with great intensity owing to their structure-dependent diverse aggregation properties, which are highly relevant in biological applications.[6,7] In the recent past, a large number of papers have appeared on different types of amphiphilic macromolecules, suggesting that several important physical properties (critical aggregation concentration, stability, and particle size) of the polymeric aggregates are more suitable for biological application than the small-molecule surfactants. Nevertheless, primarily the solvophobic collapse is the main driving force even for different polymeric structures. Thus, although extensive progress has been made toward imparting functional aspects to polymeric aggregates in terms of their encapsulation property, stimuli responsiveness,[8,9] and targeting ability, the tools to manipulate structural aspects have not been moved forward to a great extent from the classical small-molecule surfactants. In a quest to have more command on structural aspects of amphiphilic aggregates, directional supramolecular interactions such as π-stacking have been employed in conjunction with amphiphilicity in a number of recent papers relating chromophore-conjugated amphiphiles.[10,11] Examples include perylene bisimide,[12,13] porphyrin,[14,15] fullerene,[16,17] naphthalene diimide,[18−21] and other chromophore-conjugated systems.[22−25] Further mixed assembly of two different amphiphiles containing complementary aromatic donor and acceptor chromophores has also been studied in great detail.[26−32] Apart from precisely defined structure formation, these systems also offer the opportunity to extract exciting photophysical properties in the aggregated state,[12,13] which are highly desirable for their utility in imaging or sensing applications. We envisioned that structural diversity of π-conjugated amphiphiles can be enhanced if they are linked with suitable functional groups to involve directional H-bonding interaction in the self-assembly process. With this broader aim, we have recently examined aqueous self-assembly of a naphthalene diimide (NDI-2)-conjugated bola-amphiphile[33] (Scheme 1) that contains two hydrazide units for H-bonding interaction. It showed vesicular assembly by simultaneous operation of H-bonding (among the hydrazide units) and π-stacking (among the NDI chromophores). The existence of H-bonding-mediated self-assembly of abiotic units in aqueous medium is rather uncommon, and our investigation revealed

Received: January 8, 2014
Revised: January 31, 2014
Published: February 5, 2014

Scheme 1. Structures of the Two NDI-Conjugated Amphiphiles

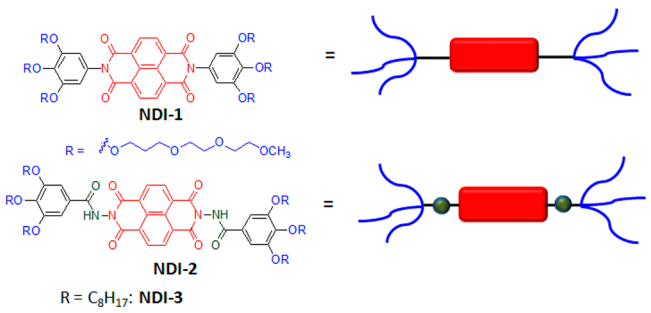

the specific location of the H-bonding units was essential for protecting them from bulk water and to remain H-bonded among themselves. The vesicular membrane also showed a unique property of very efficient intercalation of electron-rich pyrene or its derivatives by charge-transfer (CT) interaction among the pyrene and NDI chromophores. These interesting features of this system raised the question about the actual role played by H-bonding among the hydrazide units on the self-assembly and intercalation properties of NDI-2.[33] To understand that in detail, herein we have studied self-assembly of NDI-1 (Scheme 1) and compared its aggregation properties as well as guest intercalation affinity with those of NDI-2 to shed light on the specific role of H-bonding in self-assembly and co-assembly with electron-rich chromophores.

RESULTS AND DISCUSSION

Synthesis. Synthesis of NDI-1 is depicted in Chart 1. Commercially available trihydroxymethyl benzoate (**1**) was

Chart 1. Synthesis of NDI-1[a]

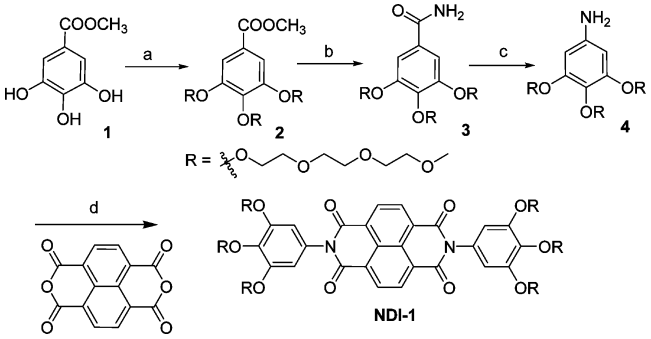

[a]Reagents and conditions: (a) R-Ts, K_2CO_3, KBr, CH_3CN, 80 °C, 95%; (b) aqueous NH_3, MeOH, rt, 12 h, 80%; (c) Br_2, KOH, 12 h, 90 °C, quantitative yield; (d) DMF, 140 °C, 80%.

alkylated with tosylate derivatives of monomethoxytriethylene glycol to produce compound **2**, which was converted to amide derivative **3** by reacting with ammonia, and then Hoffman's degradation produced amine derivative **4**. It was then reacted with naphthalenetetracarboxylic acid bis-anhydride to get the desired NDI-1, which was purified by column chromatography and isolated in 80% yield. It was structurally characterized by ^{1}H NMR and HRMS (ESI). Synthesis of NDI-2 has been reported by us elsewhere.[33]

Self-Assembly Studies. The self-assembly of NDI-1 and that of NDI-2 were compared by solvent-dependent UV−vis studies (Figure 1a). Going from THF to water, in both cases the absorption spectra showed hypochromic shift with a concomitant red shift, suggesting offset π-stacking among the NDI chromophores.[34,35] Furthermore, the intensity of the band corresponding to S_0-S_1 (λ_{max} = 376 nm) was found to be weaker than that for S_0-S_2 (λ_{max} = 356 nm) transition, confirming π-stacking. Interestingly, even in THF, a similar observation was made for NDI-1, whereas NDI-2 showed a reverse trend indicating a higher propensity of aggregation for NDI-1 so that it also shows the signature of π-stacking even in a "good" solvent such as THF. This was further confirmed by the emission spectra (Figure 1b), which show an intense excimer band[36] (λ_{em} ~ 530 nm) for NDI-1 in both THF and water, indicating aggregation in both solvents but perhaps to different extents. On the other hand, for NDI-2 the emission intensity is negligible in THF, which is attributed to an inherent low quantum yield of monomeric NDI. However, a blue-shifted (compared to the excimer band in NDI-1) band is detectable in H_2O with vibronic fine structure that has been noted for J-aggregated NDI chromophores.[36]

To further compare their aggregation, a concentration-dependent UV−vis study was carried out with NDI-1 in water (Figure 2), which shows no significant change in the absorption spectra with dilution at least until 6.5×10^{-6} M, suggesting very low critical aggregation concentration. As the absorption intensity below this concentration became very low and was significantly affected by the baseline intensity arising out of the scattering that is common in a colloidal solution, no interpretation has been made with those data. On the other hand, the same experiment with NDI-2 suggests disassembly below 0.5 mM.[33]

Temperature-variable UV−vis studies further confirmed significant difference in their aggregation property. When a solution of NDI-1 was heated to 95 °C, no change was observed in its absorption spectra (Figure 3a), revealing extremely high thermal stability. On the other hand, for NDI-2, the signature of disassembly was evident at ~65 °C from the reversal of peak intensities (Figure 3b) for S_0-S_1 and S_0-S_2 transitions.

Interestingly, around the same temperature the baseline intensity also increased (Figure 3b) due to the scattering, indicating macroscopic precipitation of the sample. Thus, this can be assigned as the lower critical solution temperature (LCST) of NDI-2. To quantify this, we have plotted the scattering-induced absorption at 600 nm for both chromophores as a function of temperature, which clearly shows (Figure 3c) the presence of LCST for NDI-2 at ~65 °C, whereas no such phenomenon is noted for NDI-1. Furthermore, we have plotted the normalized ratio of the S_0-S_1 and S_0-S_2 peak intensities for both chromophores as a function of temperature in Figure 3d, which clearly shows an inflection point at LCST and thus confirms the LCST observed in the case of NDI-2 is indeed related to the disassembly of the aggregates. On the basis of the observation described above, it is proposed that self-assembly of NDI-1 is stronger than that of NDI-2 possibly due to the absence of the hydrophilic hydrazide groups, which makes NDI-1 more hydrophobic in nature. However, at elevated temperature when the H-bonds are dissociated among the hydrazides, NDI-2 precipitates out due to denaturation-induced exposure of the hydrophobic NDI chromophore. However, for NDI-1 no such observation was made because of its much stronger propensity for self-assembly compared to NDI-2.

dx.doi.org/10.1021/la500089b | Langmuir 2014, 30, 1969−1976

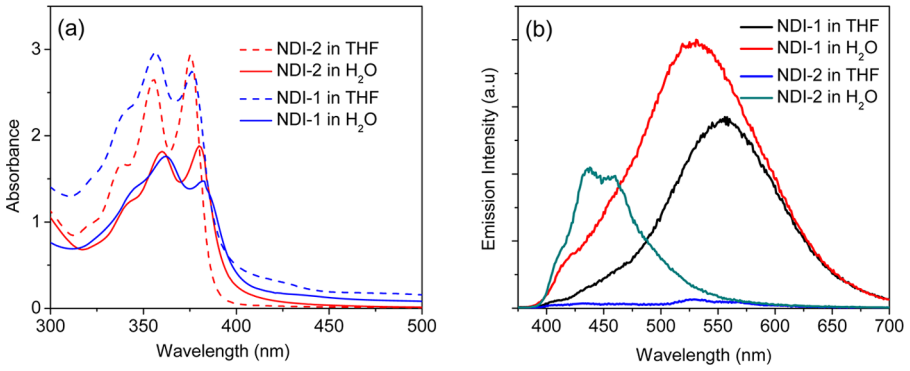

Figure 1. Solvent-dependent UV−vis (a) and emission (b) spectra. c = 1.0 mM.

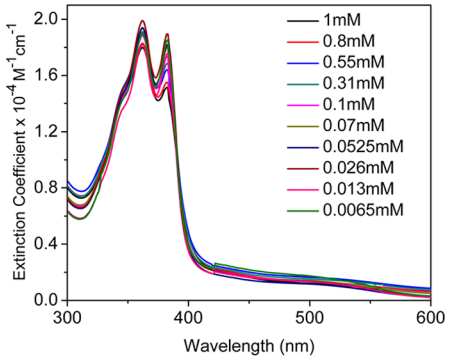

Figure 2. Concentration-dependent UV−vis absorption spectra of NDI-1 in water.

Well-defined secondary structure of a protein is generally denatured in the presence of a reagent such as urea,[37,38] which can interact with the amide groups involved in H-bonding. As the present system is primarily concerned with the role of H-bonding on self-assembly, we examined the self-assembly of NDI-1 and NDI-2 by comparing the change in their absorption spectra (Figure 4) in the presence of urea. In the presence of excess urea (2.25 M), the absorption spectra of NDI-2 show no signature of π-stacking and the presence of monomeric dye. This clearly suggests the π-stacking in this case is heavily dependent on the H-bonding among the hydrazide units. On the contrary, for NDI-1, in the presence of the same amount of urea, no change is noted for the S_0-S_1/S_0-S_2 intensity ratio, confirming intact π-stacking and thus no involvement of H-bonding in this case as expected due to the absence of any hydrazide groups.

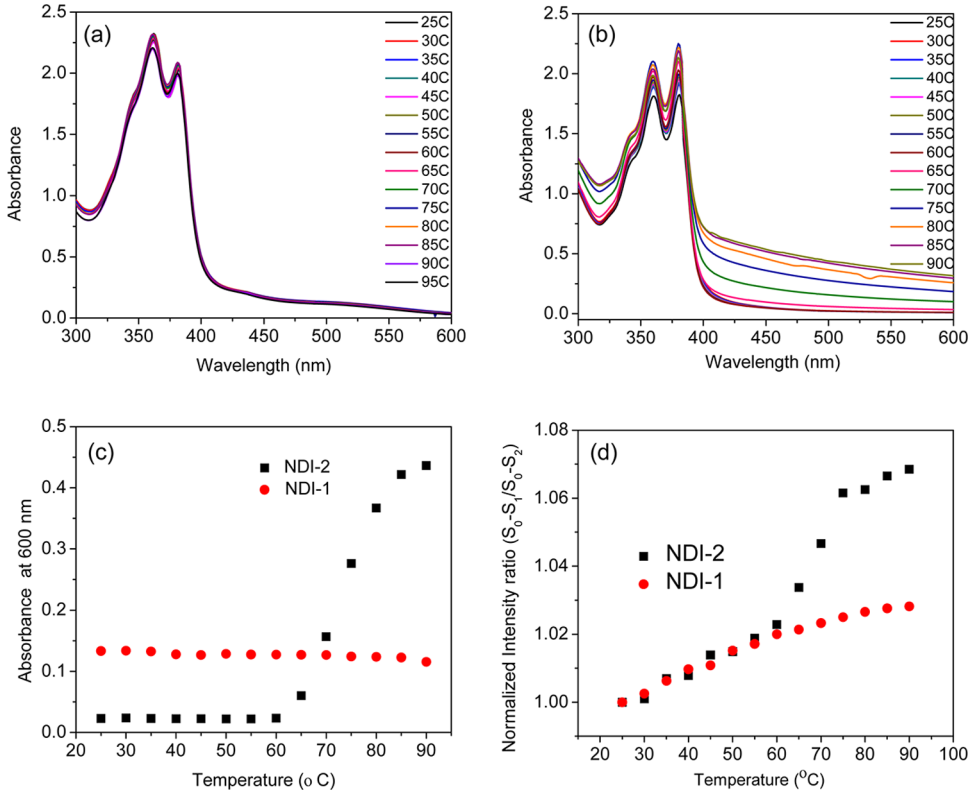

Figure 3. Variable-temperature UV−vis spectra of NDI-1 (a) and NDI-2 (b) in water (c = 1.0 mM); (c) variation of the absorbance at 600 nm as a function of temperature for both chromophores; (d) variation of the normalized (lowest temperature values were fixed to 1.0 for both chromophores) ratio of S_0-S_1/ S_0-S_2 peak intensities as a function of temperature for NDI-1 and NDI-2.

dx.doi.org/10.1021/la500089b | *Langmuir* 2014, 30, 1969−1976

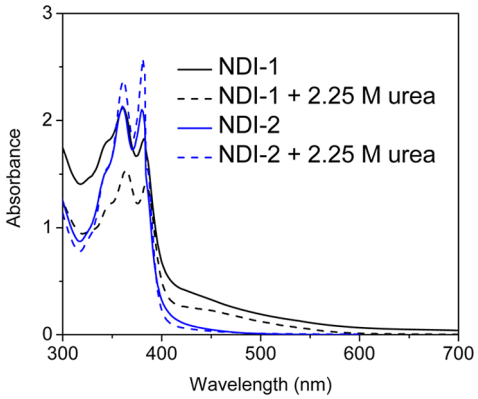

Figure 4. Effect of urea on the UV–vis absorption spectra of NDI-1 and NDI-2 in water (c = 1.0 mM). Diminished intensity of NDI-1 bands in the presence of urea may be related to shifting of the equilibrium more toward aggregates due to salting-out effect.

So far, the experimental results described primarily reveal the contrast between the two amphiphiles in terms of their interchromophoric interaction. Furthermore, we examined the macroscopic nature of the self-assembly of NDI-1 by transmission electron microscopic (TEM) studies. Figure 5a shows the presence of hollow spheres with average diameter in the range of 30–40 nm, revealing the formation of vesicles. The morphology and sizes are very similar to those reported for NDI-2,[33] and hence, similarly, it could be assumed here also that, initially, the NDI-1 molecules form a 1-D stack by $\pi-\pi$ interaction among the NDI chromophores, which then forms a vesicle, a closed membranous structure, to avoid unfavorable edge interaction of the hydrophobic NDI to water, as shown in Figure 5b. The nature of the assembly is confirmed by powder XRD, which shows a sharp peak in the small-angle region, corresponding to d = 43.2 Å, as depicted in Figure 5c. This value closely matched the theoretically estimated length of extended NDI-1 (38 Å) as shown in Figure S1 of the Supporting Information. The presence of π-stacking was also validated by the XRD data, showing a signature peak for $\pi-\pi$ stacking corresponding to d = 3.6 Å, as evident from Figure 5c. Dynamic light scattering studies confirmed unimodal size distribution (Figure 5d), although the average hydrodynamic diameter (D_h) was found to be slightly bigger than that estimated from TEM images. This is related to the effect of drying of the samples in the TEM studies.[39]

Donor Intercalation. In a previous paper on vesicular assembly of NDI-2,[33] we showed that the membrane containing electron-deficient NDI could intercalate electron-rich pyrene by virtue of strong donor (D)–acceptor (A) CT interaction.[40] Intriguingly, we noted that the intercalation resulted in fusion of the membrane, leading to slow gelation, which was attributed to the consequence of additional strain imposed by H-bonding among the hydrazide groups. As a continuation of the previous

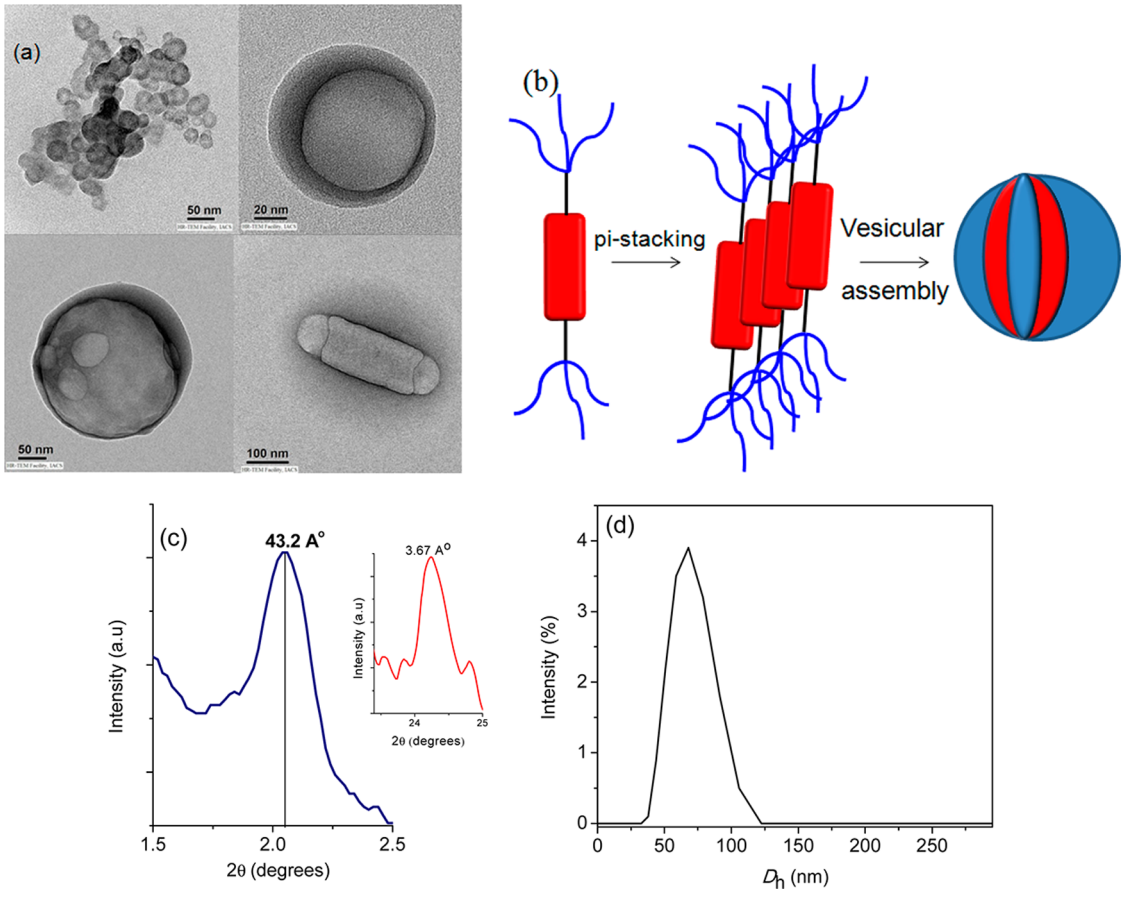

Figure 5. (a) TEM images of NDI-1 vesicular assembly by π-stacking among the chromophores as shown in panel b. The relatively bigger structures (diameter = 100–200 nm) and also the elongated structure observed in the top-right and bottom panels possibly originate from the fusion of the smaller spherical vesicles. (c) Powder XRD pattern (inset shows wide-angle selected region) of dried sample prepared from aqueous solution of NDI-1. (d) Particle size distribution as obtained from DLS for NDI-1 in water (c = 1.0 mM).

dx.doi.org/10.1021/la500089b | Langmuir 2014, 30, 1969–1976

study, another donor molecule, namely, 1,8-dimethoxynaphthalene (DMN), was investigated, which failed to form a strong CT complex with NDI-2, as evident from the UV−vis spectra given in Figure 6.

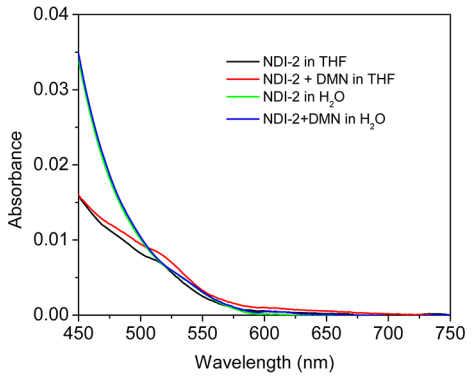

Figure 6. Solvent-dependent UV−vis absorption spectra of NDI-2 + DMN (1:1). c = 2.0 mM.

Therefore, it was comprehended that besides the nature of acceptor, the structure of the donor molecule also plays a critical role in the formation of the intercalated CT complex. Due to the poorer donating ability of DMN compared to that of pyrene, DMN is perhaps unable to intercalate within the NDI-2 assembly, resulting in a negligible CT complexation between the two. To further examine the utility of this noncovalent membrane functionalization, we attempted to intercalate a pyridine-functionalized pyrene derivative (Py-1, Figure 7) in the NDI-2 membrane in acidic pH, wherein Py-1 is soluble on its own.

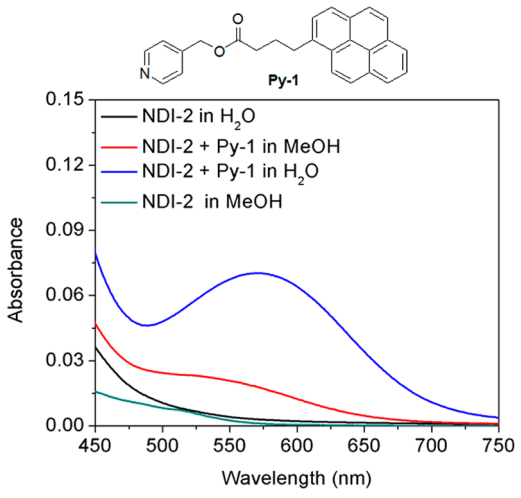

Figure 7. Solvent-dependent UV−vis absorption spectra of NDI-2 + Py-1 (1:1) and NDI-2. c = 5.0 mM. The structure of Py-1 is shown at the top.

An equimolar mixture of NDI-2 and Py-1 produced a green solution in water, suggesting intercalation and CT complex formation, which was confirmed by the appearance of a new absorption band at 565 nm in the UV−vis spectra (Figure 7).

We carried out the DLS and zeta-potential characterization (Figure 8a) of the Py-intercalated NDI-2 as a function of time to check any effect of intercalation on morphology transition. In the presence of Py-1, the hydrodynamic diameter of NDI-2 vesicles increased from ∼80 to 350−400 nm over 3 days and then remained constant. Although the size increased significantly, the nature of the aggregates remained vesicular, as has been confirmed from static light scattering (SLS) measurements, which provided a radius of gyration (R_g) value of 171 nm (Figure 8b) and an R_g/R_h ($D_h/2$) value of 1.06 (approximately unity), confirming hollow spherical morphology.[41−43] Further TEM images of the aged mixed solution showed (Figure 8c) the presence of hollow spherical particles, confirming retention of vesicular morphology. We believe that due to the donor intercalation the membrane expanded to release the strain imposed by H-bonding among the hydrazides in the intercalated state and that might have resulted in the fusion of a few vesicles to produce vesicles of larger diameter. Interestingly, the zeta-potential value concomitantly diminished from +26 mV to +2.5 mV with increasing time.[44] The positive value further confirms donor intercalation induced decoration of the membrane surface with positively charged pyridinium ion in acidic pH. However, with time as the particle size increases, the charge density reduces and thus the zeta-potential values show a descending order. On storage of the sample for more than even 7 days, no sign of generation of fibrous structure or hydrogel was noted, even at higher concentrations, unlike the previous report on pyrene intercalation. This could be attributed to the repulsion among the positively charged vesicles. To check if the charge of the nanoaggregates/pH has any role in initiating gel formation, alkali solution (0.01 mM NaOH) was gradually added to the solution of 10 mM CT complex, but the resulting solution did not show any gel formation either. Rather, after a measured amount of NaOH addition (300 μL), a hazy suspension resulted, subsequently from which a reddish precipitate settled at the bottom of the vial (Supporting Information Figure S2), possibly due to the greater hydrophobicity as a result of deprotonation of the pyridine groups.

The association constant for this complex was determined to be 4.9 × 10^2 M^{-1} from the concentration-dependent UV−vis spectra (Supporting Information Figure S3).[45,46] To tune the amount of surface functionalization with the positively charged Py-1, the amount of intercalator was varied with a fixed NDI-2 concentration. This produced a series of green solutions for which the absorption spectra were recorded, which showed a linear relationship of the CT-band as a function of concentration of the added Py-1 (Figure 9). This indicates the CT interaction mediated donor intercalation can be used as an effective strategy for tunable surface functionalization, which may have implications in a range of biologically relevant applications.

In the previous section this intercalation phenomenon was shown to be strongly dependent on the nature of the donor, and for a weak donor this did not happen. The new question is how the CT interaction mediated intercalation is dependent on the H-bonding. Surprisingly enough, NDI-1 that lacks the hydrazide groups did not exhibit any CT-band in the presence of pyrene or its water-soluble sodium butyrate derivative in aqueous solution as observed by the UV−vis spectra of the mixture (Supporting Information Figure S4). Hence, this implies that the D−A CT interaction alone is not adequate for intercalated structure formation. Due to lack of an H-bonding group in NDI-1, the intercalated D−A stack could not be molecularly "locked" by the H-bonds among the hydrazides, as in case of NDI-2. Thus the acceptor is unable to keep any donor molecule arrested in the CT complex state in aqueous

dx.doi.org/10.1021/la500089b | Langmuir 2014, 30, 1969−1976

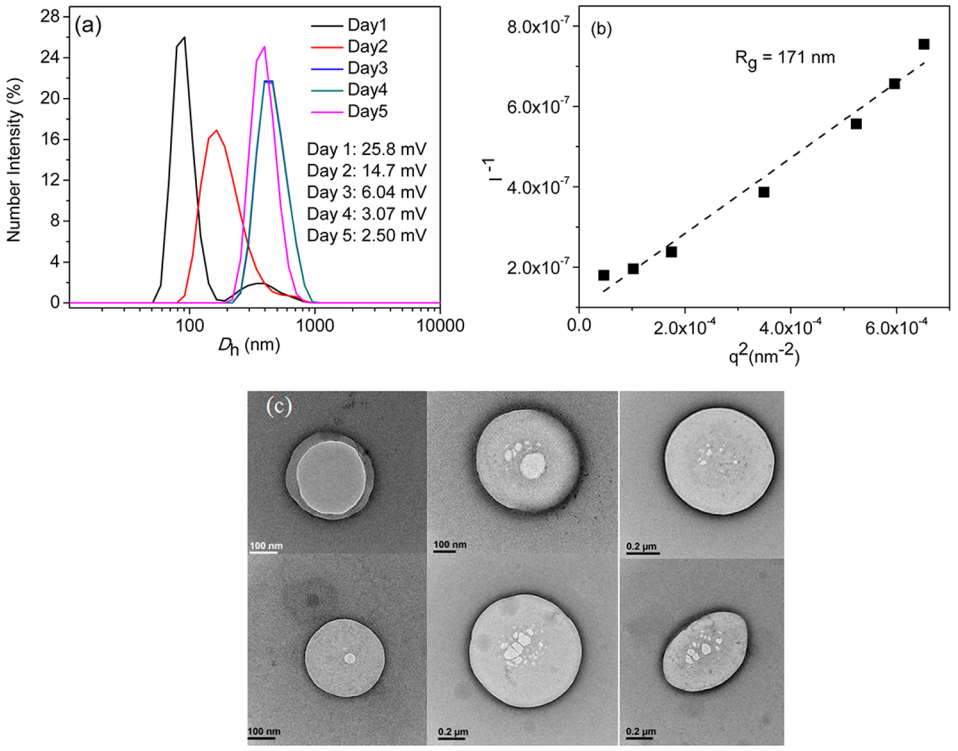

Figure 8. (a) Time-dependent DLS size distribution of the mixed aqueous solution of NDI-2 + Py-1 (1:1, c = 5.0 mM) and the corresponding zeta-potential values. (b) Zimm's plot for the determination of R_g from SLS data. (c) TEM images of the mixture after day 5.

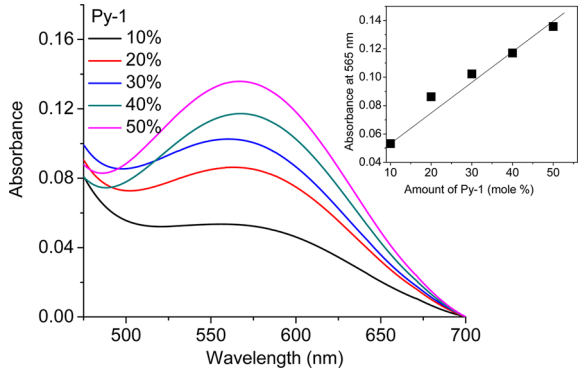

Figure 9. UV−vis absorption spectra (CT region) of NDI-2 in the presence of different amounts of Py-1. In each case total chromophore concentration = 5 mM. (Inset) Variation in absorption intensity of the CT-band at 565 nm as a function of mole percent of Py-1.

solution, although a CT color appeared in the solid state. Thus, it is evident that the donor insertion is greatly stabilized by the H-bonds in this particular system.

On the basis of the forgone discussion, it is evident that intercalation of the donor molecule is strongly correlated with H-bonding among the hydrazide units. This raises the question regarding the sequence of operation of these two noncovalent interactions. Intuitively, as the medium is water, the hydrazides are expected to be well solvated by solvent molecules, whereas the extended π-conjugated NDI or Py chromophores should have a strong tendency to form π-stacked assembly due to a hydrophobic effect. Thus, it is conceivable that the hydrophobically driven π-stacking leads to self-assembly of the NDI chromophores, which shields the hydrazide units from the bulk water due to hydrophobic effect and at the same time brings them spatially close enough to be engaged in H-bonding among themselves. To substantiate this hypothesis, we studied coassembly of NDI-3 (Scheme 1), a hydrophobic analogue of NDI-2, with pyrene in an organic solvent methylcyclohexane. In this case, no CT color was noted, in sharp contrast to the behavior of NDI-2 + Py-1 observed in water. This is because in organic solvent the H-bonding takes the lead role and thus the self-assembly is already formed by strong H-bonding, which does not allow further insertion of the donor molecule. However, in the case of water, as π-stacking leads the assembly process, initially alternate D−A assembly is formed, which then is stabilized by the H-bonding and, thus, it can be called a π-stacking-induced H-bonding, whereas in organic solvent it is H-bonding-induced π-stacking.

CONCLUSION

To summarize, we have shown comparative self-assembly studies of two amphiphilic NDI building blocks and revealed the role of H-bonding in their aggregation properties. NDI-1, which lacks the H-bonding hydrazide groups, forms stable vesicular structure in water even at very dilute condition due to π-stacking interaction among the NDI chromophores. On the other hand, a structurally similar NDI-2, which contains two hydrazide units, also forms vesicles but at relatively higher concentration and the structure is destroyed at elevated temperature, which was denoted its lower critical solution temperature. The membrane made of stacked assembly of electron-deficient NDI was tested for its ability to intercalate electron-rich pyrene or its derivatives. Surprisingly, NDI-1 did not produce any CT complex in the presence of pyrene derivatives, whereas NDI-2 could effectively intercalate pyrene and its derivatives because of the H-bonding-induced arrest of the alternate donor−acceptor stacking. The pyrene intercalation produced a modified vesicle surface with tunable presence of a functional group that was attached to the pyrene donor.

dx.doi.org/10.1021/la500089b | *Langmuir* 2014, 30, 1969−1976

Such intercalation resulted in slow enlargement of the membrane over prolonged time. Surprisingly, in organic solvents similar NDI derivatives did not show any alternate stacking with externally added pyrene. Such a striking solvent effect was attributed to a different sequence of events in water and MCH. In the case of H_2O, the assembly was primarily driven by π-stacking and the H-bonding was a consequence of that, whereas in MCH H-bonding initiated the assembly process and thus there was no scope for the pyrene chromophores to be inserted between the two NDI units before the assembly was produced.

EXPERIMENTAL SECTION

Materials and Methods. All chemicals and reagents were purchased from Sigma-Aldrich (USA) and used without any further purification unless otherwise mentioned. The solvents used for the spectroscopic studies were of spectroscopic grade. UV−vis spectra were recorded in a Perkin-Elmer Lambda 25 spectrophotometer equipped with a Peltier system for temperature-controlled experiments. Emission spectra were monitored in a Fluorolog-3 spectrophotometer, purchased from HORIBA Jobin Yvon. For measurement of the hydrodynamic size of the aggregates and the zeta potential, DLS was used, and the measurements were done in a Malvern instrument, working at a scattering angle of 173°. For the characterization of the molecule synthesized, NMR spectroscopy was utilized, and all of the NMR spectra were recorded in a Bruker DPX-300 MHz NMR spectrometer. TEM images of the formed aggregate particles were captured from JEOL-2010EX, operating at an accelerating voltage of 200 keV.

Synthesis. The synthetic procedure for the NDI-1 molecule is described in detail in the Supporting Information. NDI-2 was reported by us elsewhere.[33]

Sample Preparation. For the preparation of vesicular dispersion, a stock solution of the sample was prepared in THF, and required amounts were aliquotted for appropriate concentrations. THF was removed by air-drying, and a measured amount of water was added to make the desired concentration. The solution was then sonicated for a few minutes to make the vesicular assembly.

TEM Studies. Five microliters of aqueous solution of the sample (1.0 mM) was drop-casted on a copper grid coated with carbon mesh and left overnight for air-drying before images were captured. The same solution was also used for DLS and SLS studies.

LCST Studies by UV−Vis Spectroscopy. For LCST studies, aqueous solutions of sample (1 mM) were placed in a quartz cuvette of 0.1 cm path length and heated from 25 to 90 °C with intervals of 5 °C. Percent absorbance at 600 nm was noted at various temperatures, and 10 min of equilibration time for each temperature was allowed before the measurements were done. The absorbance at 600 nm was plotted against temperature, and LCST was obtained from the inflection point.

XRD Diffraction. XRD data were recorded on a Seifert XRD3000P diffractometer using Cu Kα radiation (α = 0.15406) with a voltage and current of 40 kV and 30 mA, respectively. For the preparation of the sample, roughly 1 mL of a concentrated solution (5.0 mM) of the sample was drop-casted repeatedly on a glass slide and left for air-drying followed by drying under vacuum, resulting in a thick film. The data were recorded from 1 to 30° with a sampling interval of 0.02°/step.

DLS and SLS Studies. For DLS studies, 1.0 mL of a 1.0 mM aqueous solution of NDI-1, NDI-2, or their CT complexes with pyrene derivatives was freshly prepared and subjected to measurement. For SLS, the same solutions prepared for DLS were used, but the measurements were done at different scattering angles (60, 80, 90, 105, and 150°). To determine the radius of gyration (R_g) using a Zimm plot, the following equation was utilized:

$$I - 1 = C(1 + R_g^2 q^2/3)$$

$I = I'\sin\theta$, I' is the intensity of scattered light, θ is the angle of scattered light, C is a constant, and q is the magnitude of the scattering wave vector given as

$$q = 4\pi n \sin(\theta/2)/\lambda_0$$

n is the refractive index of the of the liquid, and λ_0 is the wavelength of light in vacuum. The slope of the plot determines the R_g.[39,40] As we were interested in determining only the R_g, the experiment was performed with angular variation.

Determination of the Association Constant (K_a) for the CT Complex. For the determination of K_a, UV−vis spectra were recorded at different dilutions for the CT complex of NDI-2 + Py-1 (1:1). The intensity of the band at 565 nm was monitored at each dilution and, from these data K_a was determined utilizing eq 1

$$c/A = 1/(\sqrt{K_a}\varepsilon l\sqrt{A}) + 1/\varepsilon l \quad (1)$$

where c, A, ε, and l denote the concentration, absorbance, extinction coefficient, and optical path length of the cuvette, respectively. c/A is plotted against $1/A^{1/2}$, and K_a is obtained from the slope of the plot.

Fluorescence Spectroscopy. For the measurement of PL spectra of NDI-2 and NDI-1 aggregates, 1.0 mM solutions of both the compounds were prepared in THF as well as in water, and the PL spectra were recorded (λ_{ex} = 360 nm).

ASSOCIATED CONTENT

Supporting Information

Synthesis and characterization and a few additional spectral data. This material is available free of charge via the Internet at http://pubs.acs.org.

AUTHOR INFORMATION

Corresponding Authors

*(P.R.) E-mail: psupr2@iacs.res.in.
*(S.G.) E-mail: psusg2@iacs.res.in.

Notes

The authors declare no competing financial interest.

ACKNOWLEDGMENTS

P.R. thanks DST for a fellowship and funding (SR/WOS-A/CS-97/2011). M.R.M. thanks IACS, Kolkata, India, for a fellowship. P.R. also thanks Haridas Kar, PSU, IACS, for providing compound **1**. S.G. thanks SERB (SR/S1/OC-18/2012) for funding.

REFERENCES

(1) Evans, D. F.; Wennerstrom, H. *The Colloidal Domain*, 2nd ed.; Wiley-VCH: New York, 1999.
(2) Holmberg, K.; Jonsson, B.; Kronberg, B.; Lindman, B. *Surfactants and Polymers in Aqueous Solution*, 2nd ed.; Wiley: New York, 2003.
(3) O'Reilly, R. K.; Hawker, C. J.; Wooley, K. L. Cross-linked block copolymer micelles: functional nanostructures of great potential and versatility. *Chem. Soc. Rev.* **2006**, *35*, 1068−1083.
(4) Mai, Y.; Eisenberg, A. Self-assembly of block copolymers. *Chem. Soc. Rev.* **2012**, *41*, 5969−5985.
(5) Kale, T. S.; Klaikherd, A.; Popere, B.; Thayumanavan, S. Supramolecular assemblies of amphiphilic homopolymers. *Langmuir* **2009**, *25*, 9660−9670.
(6) Förster, S.; Plantenberg, T. From self-organizing polymers to nanohybrid and biomaterials. *Angew. Chem., Int. Ed.* **2002**, *41*, 688−714.
(7) Kataoka, K.; Harada, A.; Nagasaki, Y. Block copolymer micelles for drug delivery: design, characterization and biological significance. *Adv. Drug Delivery Rev.* **2001**, *47*, 113−131.
(8) Roy, D.; Cambre, J. N.; Sumerlin, B. S. Future perspectives and recent advances in stimuli-responsive materials. *Prog. Polym. Sci.* **2010**, *35*, 278−301.

(9) Chacko, R. T.; Ventura, J.; Zhuang, J.; Thayumanavan, S. Polymer nanogels: a versatile nanoscopic drug delivery platform. *Adv. Drug Delivery Rev.* **2012**, *64*, 836−851.
(10) Ryu, J.-H.; Hong, D.-J.; Lee, M. Aqueous self-assembly of aromatic rod building blocks. *Chem. Commun.* **2008**, 1043−1054.
(11) Hoeben, F. J. M.; Jonkheijm, P.; Meijer, E. W.; Schenning, A. P. H. J. About supramolecular assemblies of π-conjugated systems. *Chem. Rev.* **2005**, *105*, 1491−1546.
(12) Zhang, X.; Rehm, S.; Safont-Sempere, M. M.; Würthner, F. Vesicular perylene dye nanocapsules as supramolecular fluorescent pH sensor systems. *Nat. Chem.* **2009**, *1*, 623−629.
(13) Zhang, X.; Görl, D.; Würthner, F. White-light emitting dye micelles in aqueous solution. *Chem. Commun.* **2013**, *49*, 8178−8180.
(14) Sakurai, T.; Shi, K.; Sato, H.; Tashiro, K.; Osuka, A.; Saeki, A.; Seki, S.; Tagawa, S.; Sasaki, S.; Masunaga, H.; Osaka, K.; Takata, M.; Aida, T. Prominent electron transport property observed for triply fused metalloporphyrin dimer: directed columnar liquid crystalline assembly by amphiphilic molecular design. *J. Am. Chem. Soc.* **2008**, *130*, 13812−13813.
(15) Sakurai, T.; Tashiro, K.; Honsho, Y.; Saeki, A.; Seki, S.; Osuka, A.; Muranaka, A.; Uchiyama, M.; Kim, J.; Ha, S.; Kato, K.; Takata, M.; Aida, T. Electron- or hole-transporting nature selected by side-chain-directed π-stacking geometry: liquid crystalline fused metalloporphyrin dimer. *J. Am. Chem. Soc.* **2011**, *133*, 6537−6540.
(16) Charvet, R.; Yamamoto, Y.; Sasaki, T.; Kim, J.; Kato, K.; Takata, M.; Saeki, A.; Seki, S.; Aida, T. Segregated and alternately stacked donor/acceptor nanodomains in tubular morphology tailored with zinc porphyrin−C_{60} amphiphilic dyads: clear geometrical effects on photoconduction. *J. Am. Chem. Soc.* **2012**, *134*, 2524−2527.
(17) Muñoz, A.; Illescas, B. M.; Sánchez-Navarro, M.; Rojo, J.; Martín, N. Nanorods versus nanovesicles from amphiphilic dendrofullerenes. *J. Am. Chem. Soc.* **2011**, *133*, 16758−16761.
(18) Shao, H.; Nguyen, T.; Romano, N. C.; Modarelli, D. A.; Parquette, J. R. Self-assembly of 1-D *n*-type nanostructures based on naphthalene diimide-appended dipeptides. *J. Am. Chem. Soc.* **2009**, *131*, 16374−16376.
(19) Shao, H.; Gao, M.; Kim, S. H.; Jaroniec, C. P.; Parquette, J. R. Aqueous self-assembly of L-lysine-based amphiphiles into 1D n-type nanotubes. *Chem.−Eur. J.* **2011**, *17*, 12882−12885.
(20) Lokey, R. S.; Iverson, B. L. Synthetic molecules that fold into a pleated secondary structure in solution. *Nature* **1995**, *375*, 303−305.
(21) Kumar, M.; George, S. J. Green fluorescent organic nanoparticles by self-assembly induced enhanced emission of a naphthalene diimide bolaamphiphile. *Nanoscale* **2011**, *3*, 2130−2133.
(22) Van Nostrum, C. F.; Picken, S.; Schouten, A.-J.; Nolte, R. J. M. Synthesis and supramolecular chemistry of novel liquid crystalline crown ether-substituted phthalocyanines: toward molecular wires and molecular ionoelectronics. *J. Am. Chem. Soc.* **1995**, *117*, 9957−9965.
(23) Engelkamp, H.; Middelbeek, S.; Nolte, R. J. M. Self-assembly of disk-shaped molecules to coiled-coil aggregates with tunable helicity. *Science* **1999**, *284*, 785−788.
(24) Seo, S. H.; Chang, J. Y.; Tew, G. N. Self-assembled vesicles from an amphiphilic ortho-phenylene ethynylene macrocycle. *Angew. Chem., Int. Ed.* **2006**, *45*, 7526−7530.
(25) Chen, L.; Mali, K. S.; Puniredd, S. R.; Baumgarten, M.; Parvez, K.; Pisula, W.; Feyter, S. D.; Müllen, K. Assembly and fiber formation of a gemini-type hexathienocoronene amphiphile for electrical conduction. *J. Am. Chem. Soc.* **2013**, *135*, 13531−13537.
(26) Zhang, X.; Wang, C. Supramolecular amphiphiles. *Chem. Soc. Rev.* **2011**, *40*, 94−101.
(27) Wang, C.; Wang, Z. Q.; Zhang, X. Amphiphilic building blocks for self-assembly: from amphiphiles to supra-amphiphiles. *Acc. Chem. Res.* **2012**, *45*, 608−618.
(28) Wang, C.; Yin, S.; Chen, S.; Xu, H.; Wang, Z.; Zhang, X. Controlled self-assembly manipulated by charge-transfer interactions: from tubes to vesicles. *Angew. Chem., Int. Ed.* **2008**, *47*, 9049−9052.
(29) Wang, C.; Guo, Y.; Wang, Z.; Zhang, X. Superamphiphiles based on charge transfer complex: controllable hierarchical self-assembly of nanoribbons. *Langmuir* **2010**, *26*, 14509−14511.
(30) Liu, K.; Wang, C.; Li, Z.; Zhang, X. Superamphiphiles based on directional charge-transfer interactions: from supramolecular engineering to well-defined nanostructures. *Angew. Chem., Int. Ed.* **2011**, *50*, 4952−4956.
(31) Rao, K. V.; George, S. J. Supramolecular alternate co-assembly through a non-covalent amphiphilic design: conducting nanotubes with a mixed D−A structure. *Chem.−Eur. J.* **2012**, *18*, 14286−14291.
(32) Das, A.; Ghosh, S. Stimuli-responsive self-assembly of a naphthalene diimide by orthogonal hydrogen bonding and its coassembly with a pyrene derivative by a pseudo-intramolecular charge-transfer interaction. *Angew. Chem., Int. Ed.* **2014**, *53*, 1092−1097.
(33) Molla, M. R.; Ghosh, S. Hydrogen-bonding-mediated vesicular assembly of functionalized naphthalene-diimide-based bolaamphiphile and guest-induced gelation in water. *Chem.−Eur. J.* **2012**, *18*, 9860−9869.
(34) Bhosale, S. V.; Jani, C. H.; Langford, S. Chemistry of naphthalene diimides. *Chem. Soc. Rev.* **2008**, *37*, 331−342.
(35) Sakai, N.; Mareda, J.; Vauthey, E.; Matile, S. Core-substituted naphthalenediimides. *Chem. Commun.* **2010**, *46*, 4225−4237.
(36) Molla, M. R.; Gehrig, D.; Roy, L.; Kamm, V.; Paul, A.; Laquai, F.; Ghosh, S. Self-assembly of carboxylic acid appended naphthalene diimide (NDI) derivatives with tunable luminescent color and electrical conductivity. *Chem.−Eur. J.* **2013**, DOI: 10.1002/chem.201303379.
(37) Canchi, D. R.; Paschek, D.; García, A. E. An equilibrium study of protein denaturation by urea. *J. Am. Chem. Soc.* **2010**, *132*, 2338−2344.
(38) O'Brien, E. P.; Dima, R. I.; Brooks, B.; Thirumalai, D. Interactions between hydrophobic and ionic solutes in aqueous guanidinium chloride and urea solutions: lessons for protein denaturation mechanism. *J. Am. Chem. Soc.* **2007**, *129*, 7346−7353.
(39) Dua, J.; O'Reilly, R. K. Advances and challenges in smart and functional polymer vesicles. *Soft Matter* **2009**, *5*, 3544−3561.
(40) Kumar, N. S. S.; Gujrati, M. D.; Wilson, J. N. Evidence of preferential π-stacking: a study of intermolecular and intramolecular charge transfer complexes. *Chem. Commun.* **2010**, *46*, 5464−5466.
(41) Burchard, W. Static and dynamic light scattering from branched polymers and biopolymers. In *Light Scattering from Polymers*; Advances in Polymer Science 48; Springer Verlag: Berlin, Germany, 1983; pp 1−124
(42) Maughton, A. O.; O'Reilly, R. K. Thermally induced micelle to vesicle morphology transition for a charged chain end diblock copolymer. *Chem. Commun.* **2010**, *46*, 1091−1093.
(43) Surnar, B.; Jayakannan, M. Stimuli responsive poly(caprolactone) vesicles for dual drug delivery under the gastrointestinal tract. *Biomacromolecules* **2013**, *14*, 4377−4387.
(44) Zeta potential of spherical aggregates is determined as charge/size. Because zeta potential is inversely proportional to the size of the aggregates, hence, in our case as the size increased gradually, the zeta potential value decreased steadily as well.
(45) Nielsen, M. B.; Jeppesen, J. O.; Lau, J.; Lomholt, C.; Damgaard, D.; Jacobsen, J. P.; Becher, J.; Stoddart, J. F. Binding studies between tetrathiafulvalene derivatives and cyclobis(paraquat-*p*-phenylene). *J. Org. Chem.* **2001**, *66*, 3559−3563.
(46) De, S.; Koley, D.; Ramakrishnan, S. Folding a polymer via two-point interaction with an external folding agent: use of H-bonding and charge-transfer interactions. *Macromolecules* **2010**, *43*, 3183−3192.